

## Does the fraction of dark matter diminish with early dark energy?

Hao Wang<sup>1,2,\*</sup> and Yun-Song Piao<sup>1,2,3,4,†</sup>

<sup>1</sup>School of Fundamental Physics and Mathematical Sciences, Hangzhou Institute for Advanced Study, UCAS, Hangzhou 310024, China

<sup>2</sup>School of Physics Sciences, University of Chinese Academy of Sciences, Beijing 100049, China

<sup>3</sup>International Center for Theoretical Physics Asia-Pacific, Beijing/Hangzhou, China

<sup>4</sup>Institute of Theoretical Physics, Chinese Academy of Sciences, P.O. Box 2735, Beijing 100190, China



(Received 5 October 2022; accepted 18 September 2023; published 16 October 2023)

In prerecombination early dark energy (EDE) resolutions of the Hubble tension, the rise of Hubble constant value  $H_0$  is usually accompanied with the exacerbation of so-called  $S_8$  tension. Inspired by the swampland conjecture, we investigate what if a fraction  $f_*$  of dark matter is coupled to EDE,  $m_{\text{cdm}} \sim \exp(-c \frac{|\Delta\phi_{\text{ede}}|}{M_{pl}})$  with  $c \sim \mathcal{O}(1)$ . We perform the Markov chain Monte Carlo analysis for the relevant EDE models with PlanckCMB, BAO, Pantheon and SH0ES dataset, as well as DES-Y1 data, and find that such a fraction helps to alleviate the  $S_8$  tension. However, though  $c \gtrsim 0.1$  is allowed for a very small  $f_*$ , which suggests that a small fraction of dark matter has ever faded with EDE,  $c \sim 0$  is also consistent.

DOI: 10.1103/PhysRevD.108.083516

### I. INTRODUCTION

There is a  $5\sigma$  conflict between the Hubble constant  $H_0 \sim 67$  km/s/Mpc inferred by the Planck collaboration [1] using cosmological microwave background (CMB) data based on the  $\Lambda$ CDM model and that obtained by SH0ES in light of Cepheid-calibrated SN data,  $H_0 \sim 73$  km/s/Mpc [2], which is so-called Hubble tension [3,4], see [5–7] for reviews. Currently, it seems impossible to explain this conflict by systematic errors; thus, it has been widely thought that this tension signals new physics beyond  $\Lambda$ CDM.

The Hubble tension is possibly resolved with early dark energy (EDE) [8–10]. Here, the EDE is non-negligible only before recombination, which suppressed the sound horizon and so naturally brings a high  $H_0$  without spoiling fit to CMB and baryon acoustic oscillation (BAO) data. In particular, if an anti-de Sitter (AdS) phase existed around recombination (AdS-EDE model [11,12]), we would have the bestfit  $H_0 \simeq 73$  km/s/Mpc, which is  $1\sigma$  consistent with local  $H_0$  measurement. Recently, besides Planck data, combined analysis of CMB data have been also performed for EDE, such as Planck + SPT [13–15], Planck + ACT DR4 [16,17], Planck + ACT DR4 + SPT-3G [18–21], and Planck + BICEP/Keck [22].

In such prerecombination EDE resolutions, the rise of  $H_0$  is usually accompanied with the exacerbation of so-called  $S_8$  tension [23–25], see also [26,27], where

$$S_8 = \sigma_8 (\Omega_m / 0.3)^{1/2}, \quad (1)$$

and  $\sigma_8$  is the amplitude of matter perturbations at  $8h^{-1}$  Mpc scale. It is well known that  $S_8 \sim 0.82$  for  $\Lambda$ CDM and  $S_8 \gtrsim 0.84$  for EDE, while the local large-scale structure observations [28–30] have reported lower  $S_8 \sim 0.76$ . Recently, the resolution of  $S_8$  tension has been intensively studied, which might be completely independent of EDE, such as dark matter (DM)-DE drag [31] at low redshifts, ultralight axion as a little part of DM [32–34], decaying DM [35–37], massive neutrino [38], and also [39,40].

However, the DM physics responsible for the  $S_8$  tension might also be relevant with EDE, e.g. [41–43]. The conformal coupling of DM to EDE has been considered in Ref. [41], see also [44,45] for neutrino-assisted EDE. The conformal coupling to all matter fields was also considered in Refs. [46–49]. The coupled EDE and the impact of massive neutrinos also has been studied in Ref. [50]. The evolution of our Universe must be implemented in a UV-complete effective field theory (EFT). It has been argued in Ref. [51] that such EFTs must satisfy the *swampland distance conjecture* (SDC): the excursion of any field must comply with  $|\Delta\phi| \lesssim M_{pl}$ , or it will cause the exponential suppression of the mass of other fields in EFT. Thus it is possible that DM might be exponentially lightened (called “fading dark matter” [52]) with the evolution of EDE. However, in such an early dark sector [42], the results favored by current datasets seem conflicted with SDC.

It might be also possible that not all but only a fraction of DM is coupled EDE. In this paper, we will investigate such a coupling in axionlike EDE and AdS-EDE models, respectively. In Sec. II, we comment on the correlation of  $S_8 - H_0$ , and outline our setup in Sec. III. In Secs. IV and V, we perform the Markov chain Monte Carlo (MCMC)

\*wanghao187@mails.ucas.ac.cn

†yspiao@ucas.ac.cn

analysis with PlanckCMB, BAO, Pantheon and SH0ES datasets, as well as a full DES-Y1 dataset, and report our results. We conclude in Sec. VI.

## II. $S_8 - H_0$ IN EDE

It is well known that the Planck dataset strictly set the angular scale

$$\theta_{\text{CMB}} = \frac{r_s}{D_A} \sim r_s H_0, \quad (2)$$

where  $D_A = \int_0^{z_*} \frac{dz}{H(z)}$  is the angular radius to the last scattering surface,  $r_s = \int_{z_*}^{\infty} \frac{c_s}{H(z)} dz$  is the sound horizon, and  $z_*$  is the redshift of last scattering. In prerecombination EDE setup,  $r_s$  is suppressed (see [53] for recent result) so that we have a high  $H_0$  in light of (2). Recently, the relevant EDE models have widely studied e.g. [10–12, 54–65], and [46, 48, 66–69]; see also its effects on cosmic birefringence [70, 71] and gravitational waves background [72, 73].

It has been shown in Ref. [74] that even if the state equation  $w(z)$  of DE after recombination evolved with the redshift  $z$ , its rise for the bestfit  $H_0$  is also negligible. However, though the postrecombination beyond- $\Lambda$ CDM modification seems difficult to resolve the Hubble tension, it is still worth exploring, e.g. [75–88], see also [89–91] (the physics of our Universe might be abruptly interrupted at redshifts  $z = 0.01$  in the past), or it might be also possible that the flat  $\Lambda$ CDM model is breaking down [92–94].

In prerecombination EDE resolutions, the cosmological parameters must shift with  $\delta H_0$ , particularly the shift of  $\omega_m = \Omega_m h^2$  scales approximately [12]

$$\delta\omega_m \simeq 2 \frac{\delta H_0}{H_0} \omega_m, \quad (3)$$

since the PlanckCMB + BAO dataset requires  $\omega_m \sim H_0^2$  (or  $\Omega_m \sim \text{const}$ ). The dustlike matter will cluster in the matter-dominated era, so higher  $H_0$  will proportionally bring a higher  $S_8$ . Thus, the EDE will inevitably suffer from the exacerbation of  $S_8$  tension, see Fig. 1.

In the standard EDE +  $\Lambda$ CDM model, all DM not only participates in the background evolution of the Universe but also is responsible for perturbation growth, which naturally results in (3) and so suggests exacerbated  $S_8$  tension for EDE. There might be, however, other possible matter forms or coupling which can break the correlation between  $S_8$  and  $\omega_m$ . In this sense, the  $S_8$  tension is actually an opportunity of understanding CDM physics.

## III. DARK MATTER FRACTIONALLY COUPLED TO EDE

The SDC suggests [51] that any EFT is only valid in field space bounded by the Planck scale,  $|\Delta\phi| < M_{pl}$ , and its breakdown that occurs at Planckian field excursions

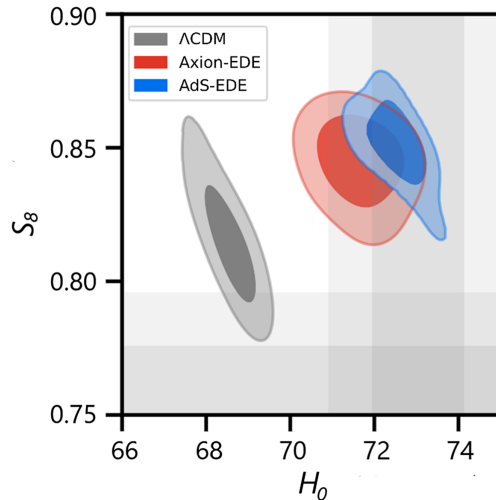


FIG. 1. The  $S_8 - H_0$  contour for  $\Lambda$ CDM, axionlike EDE and AdS-EDE models. The shadows correspond to the  $1\sigma$  and  $2\sigma$  regions of  $H_0$  in light of recent SH0ES  $H_0 = 73.04 \pm 1.04$  km/s/Mpc [2] and  $S_8$  in light of KiDS + VIKING-450 + DES-Y1 constraint  $S_8 = 0.755 \pm 0.02$  [28], respectively. It is clearly seen that the EDE also proportionally lifts  $S_8$  while lifting  $H_0$ .

is encoded in the mass spectrum of other fields,  $m \sim \exp(-c|\Delta\phi|/M_{pl})$ , where  $c \simeq \mathcal{O}(1)$ , see [95, 96] for reviews.

Inspired by the SDC, we consider the couple of DM with EDE. The dark matter is modeled as a population of nonrelativistic Dirac fermions  $\psi$ ,

$$\mathcal{L}_{\text{int}} \sim -m_{\text{cdm}}(\phi)\bar{\psi}\psi, \quad (4)$$

$$m_{\text{cdm}}(\phi) = f_* m(\phi) + (1 - f_*) m_i, \quad \text{with } 0 \leq f_* \leq 1, \quad (5)$$

$$m(\phi) = m_i e^{-c(\frac{|\Delta\phi| - \phi_*}{M_{pl}})}, \quad \text{for } |\Delta\phi| \geq \phi_*. \quad (6)$$

where  $m_i = \text{const}$  is the initial mass of DM,  $|\Delta\phi| = |\phi - \phi_i|$  (see Fig. 2),  $\phi_*$  signals the insensitivity of DM on a shift of  $\phi$  within  $|\Delta\phi| < \phi_*$ , and  $c$  is the coupling intensity. Here, when  $c = 0$ , we have  $m_{\text{cdm}} = m_i$  (the standard EDE +  $\Lambda$ CDM model is recovered).

In the nonrelativistic limit, we have  $\rho_{\text{cdm}} = n m_{\text{cdm}}(\phi)$ , so

$$\rho_{\text{cdm}} = n f_* m(\phi) + n(1 - f_*) m_i, \quad (7)$$

with  $n$  being the number density, which suggests that  $f_*$  is actually equivalent to the fraction of DM coupled to EDE.

Here, we follow Ref. [42]. The evolution of EDE is rewritten as  $\phi'' + 2\mathcal{H}\phi' + a^2 V_\phi = -a^2 \frac{d\rho_{\text{cdm}}}{d\phi}$ , while the continuity equation for DM is

$$\rho'_{\text{cdm}} + 3\mathcal{H}\rho_{\text{cdm}} = \phi' \frac{d\rho_{\text{cdm}}}{d\phi}, \quad (8)$$

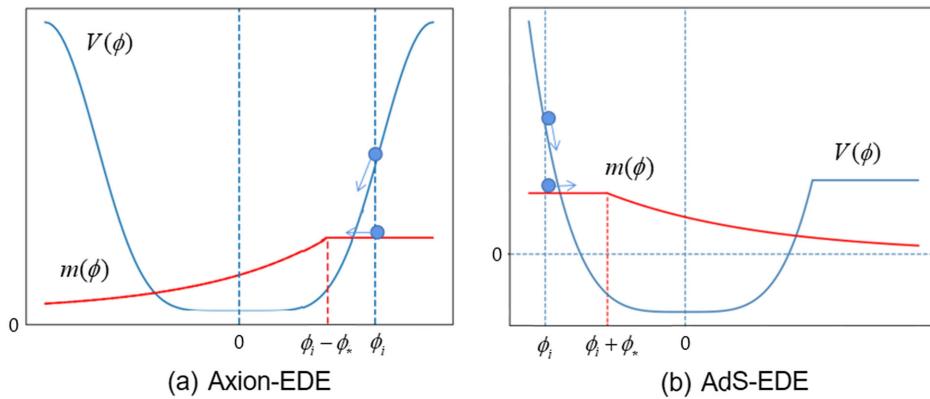


FIG. 2. A sketch of the EDE potential  $V(\phi)$  and  $m(\phi)$  in axionlike EDE and AdS-EDE models, respectively. Initially the field sits at  $\phi_i$ , after its excursion  $|\Delta\phi| > \phi_*$ , the mass of DM will be exponentially lightened with the evolution of  $\phi$ .

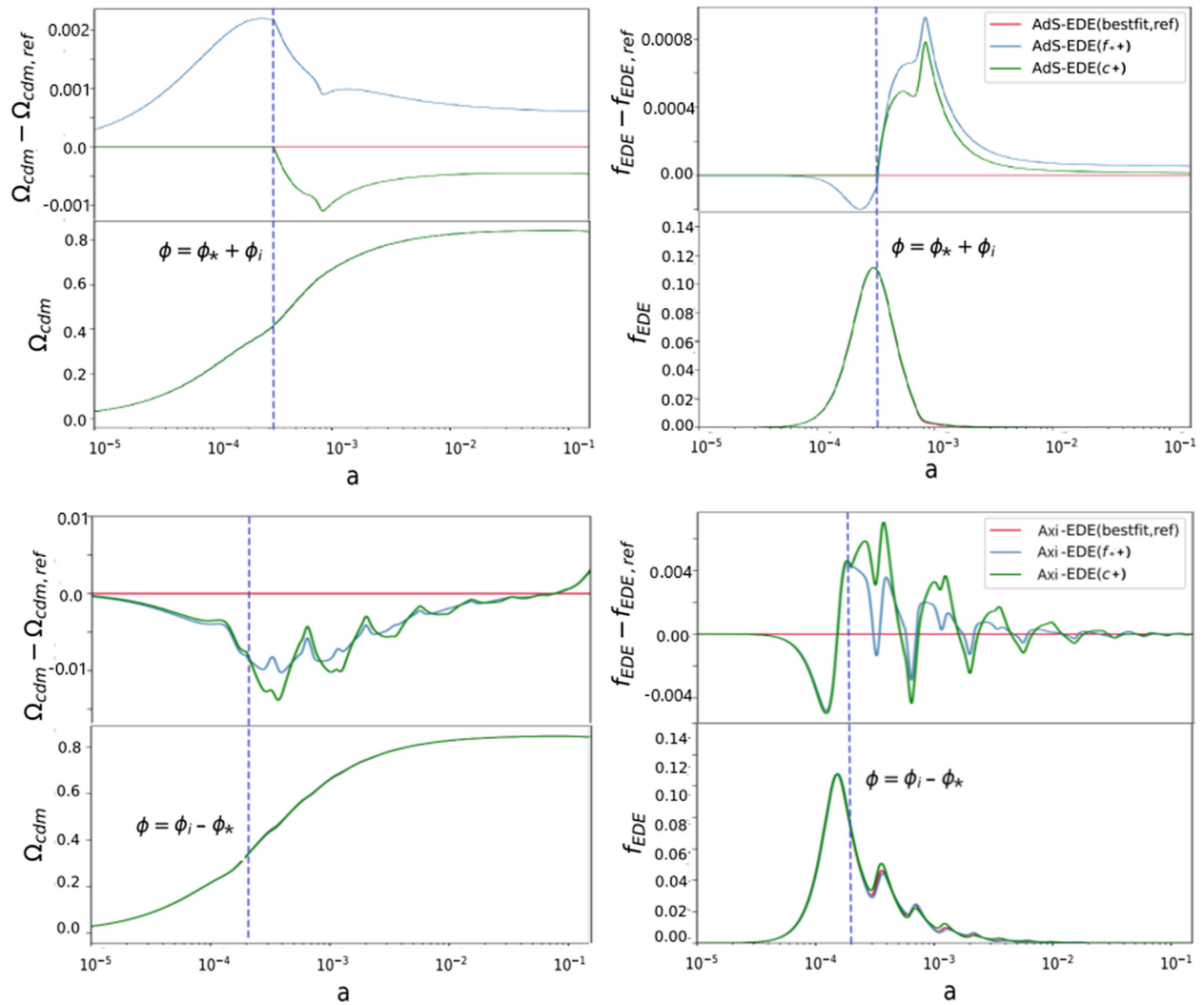


FIG. 3. The evolution of  $f_{\text{EDE}}$  and  $\Omega_{\text{cdm}}$  for both axion-EDE and AdS-EDE (red curves). The blue and green curves show the effect of increasing the parameters  $f_*$  and  $c$  by 10% from the bestfit values of EDE models. We display the discrepancies of them in the upper panels to clarify the difference. The vertical purple dashed lines correspond to the  $|\phi - \phi_i| = \phi_*$  when the dark matter begins to couple to EDE.

where the *prime* is the derivative with respect to  $d\eta = dt/a$ , and  $\mathcal{H} = a'/a$ . Integrating Eq. (8), we have

$$\rho_{\text{cdm}}(a) = \frac{3M_{pl}^2 H_0^2 \Omega_{\text{cdm}}}{a^3} \left[ 1 - f(\phi_0) + \frac{m(\phi)}{m(\phi_0)} f(\phi_0) \right], \quad (9)$$

where  $f(\phi) = \frac{m(\phi)f_*}{m(\phi)f_* + m_i(1-f_*)}$ , and  $\phi_0$  is the present-day value of  $\phi$ .

The axionlike EDE has a potential of the form  $V(\phi) = m^2 f^2 [1 - \cos(\phi/f)]^n$  motivated by higher-order instanton corrections in string theory. In this model, the field rolls

down at about  $z \sim 3000$ , oscillates and settles down the bottom of the potential. In the axionlike EDE model, see Fig. 2(a),  $\phi - \phi_i < 0$  for  $\phi_i > 0$ , so  $d\rho_{\text{cdm}}/d\phi = c\rho_{\text{cdm}}f(\phi)/M_{pl}$ . The scalar field will eventually settle at the bottom of its potential, so  $\phi_0 = 0$ .

The equations of motion for linear perturbations of the scalar field and dark matter may be derived from the variation of the action with respect to the scalar field perturbations and the conservation of the perturbed joint stress-energy tensor  $\nabla_\mu T^\mu_\nu = 0$ . In the synchronous gauge, with  $\rho_{\text{cdm}}$  in Eq. (9), the perturbation equations adapted are

TABLE I. Mean (bestfit) values of  $\Lambda$ CDM and axionlike EDE with and without coupling (6) in fit to the baseline, baseline + SH0ES and the baseline + SH0ES + DES-Y1 datasets, respectively.

$\Lambda$ CDM			
Parameters	Baseline	Baseline + $H_0$	Baseline + $H_0$ + DES-Y1
$100\omega_b$	$2.238(2.239) \pm 0.014$	$2.252(2.249) \pm 0.013$	$2.257(2.263) \pm 0.014$
$\omega_{\text{cdm}}$	$0.1179(0.1177) \pm 0.0012$	$0.1182(0.1184) \pm 0.0008$	$0.1172(0.1167) \pm 0.0007$
$H_0$	$68.18(68.13) \pm 0.54$	$68.21(68.16) \pm 0.39$	$69.13(69.48) \pm 0.38$
$\ln(10^{10}A_s)$	$3.028(3.042) \pm 0.013$	$3.052(3.052) \pm 0.015$	$3.046(3.048) \pm 0.015$
$n_s$	$0.9686(0.9687) \pm 0.0044$	$0.9691(0.9686) \pm 0.0035$	$0.9705(0.9769) \pm 0.0036$
$\tau_{\text{reio}}$	$0.075(0.068) \pm 0.013$	$0.0595(0.0594) \pm 0.0073$	$0.0593(0.0618) \pm 0.0080$
$S_8$	$0.8141(0.8142) \pm 0.012$	$0.8140(0.8156) \pm 0.0098$	$0.8067(0.8019) \pm 0.0103$
Axion-EDE (uncoupled)			
Parameters	Baseline	Baseline + $H_0$	Baseline + $H_0$ + DES-Y1
$100\omega_b$	$2.255(2.258) \pm 0.022$	$2.280(2.286) \pm 0.020$	$2.277(2.268) \pm 0.017$
$\omega_{\text{cdm}}$	$0.1272(0.1299) \pm 0.0045$	$0.1296(0.1344) \pm 0.0039$	$0.1324(0.1303) \pm 0.1129$
$H_0$	$70.60(71.60) \pm 1.3$	$71.20(72.50) \pm 1.10$	$72.40(72.24) \pm 0.42$
$\ln(10^{10}A_s)$	$3.065(3.064) \pm 0.015$	$3.067(3.079) \pm 0.015$	$3.066(3.066) \pm 0.016$
$n_s$	$0.9812(0.9880) \pm 0.0080$	$0.9865(0.9930) \pm 0.0071$	$0.9946(0.9891) \pm 0.0035$
$\tau_{\text{reio}}$	$0.0680(0.068) \pm 0.013$	$0.0578(0.0600) \pm 0.0072$	$0.0680(0.0671) \pm 0.0096$
$f_{\text{ede}}$	$0.050(0.058) \pm 0.022$	$0.104(0.142) \pm 0.032$	$0.105(0.122) \pm 0.030$
$\log_{10} a_c$	$-3.737(-3.696) \pm 0.102$	$-3.606(-3.580) \pm 0.077$	$-3.780(-3.741) \pm 0.064$
$S_8$	$0.8380(0.8420) \pm 0.015$	$0.8380(0.8495) \pm 0.0130$	$0.8280(0.8298) \pm 0.0108$
Axion-EDE			
Parameters	Baseline	Baseline + $H_0$	Baseline + $H_0$ + DES-Y1
$100\omega_b$	$2.272(2.270) \pm 0.019$	$2.284(2.286) \pm 0.020$	$2.290(2.282) \pm 0.017$
$\omega_{\text{cdm}}$	$0.1281(0.1283) \pm 0.0036$	$0.1306(0.1290) \pm 0.0020$	$0.1251(0.1236) \pm 0.0011$
$H_0$	$70.21(71.25) \pm 1.20$	$70.87(71.66) \pm 0.63$	$70.83(70.14) \pm 0.57$
$\ln(10^{10}A_s)$	$3.062(3.046) \pm 0.018$	$3.060(3.051) \pm 0.013$	$3.051(3.031) \pm 0.013$
$n_s$	$0.9832(0.9837) \pm 0.0065$	$0.9889(0.9834) \pm 0.0056$	$0.9824(0.9786) \pm 0.0033$
$\tau_{\text{reio}}$	$0.0573(0.0574) \pm 0.0018$	$0.0576(0.0571) \pm 0.0064$	$0.0553(0.0487) \pm 0.0047$
$f_{\text{ede}}$	$0.102(0.081) \pm 0.0015$	$0.116(0.101) \pm 0.017$	$0.068(0.055) \pm 0.008$
$\log_{10} a_c$	$-3.759(-3.821) \pm 0.198$	$-3.748(-3.841) \pm 0.137$	$-3.585(-3.602) \pm 0.073$
$c$	$0.310(-0.115) \pm 0.490$	$0.289(-0.129) \pm 0.472$	$-0.015(-0.012) \pm 0.082$
$\phi_*$	$0.312(0.359) \pm 0.131$	$0.305(0.361) \pm 0.147$	$0.321(0.406) \pm 0.127$
$f_*$	$0.185(0.237) \pm 0.239$	$0.183(0.222) \pm 0.229$	$0.521(0.860) \pm 0.289$
$S_8$	$0.8383(0.8425) \pm 0.014$	$0.8451(0.8438) \pm 0.0112$	$0.8263(0.8186) \pm 0.0122$

$$\ddot{\delta\phi} + 2aH\dot{\delta\phi} + \left(k^2 + a^2 \frac{d^2V}{d\phi^2}\right)\delta\phi + \frac{\dot{h}}{2}\dot{\phi} = -a^2 \frac{d\rho_{\text{cdm}}}{d\phi} \delta_c, \quad (10)$$

where the fractional dark matter density perturbation  $\delta_c \equiv \delta\rho_{\text{cdm}}/\rho_{\text{cdm}}$  and  $h$  is the trace of the spatial metric perturbation, and

$$\dot{\delta}_c + \theta + \frac{\dot{h}}{2} = \frac{1}{\rho_{\text{cdm}}} \frac{d\rho_{\text{cdm}}}{d\phi} \dot{\delta\phi} \quad (11)$$

with

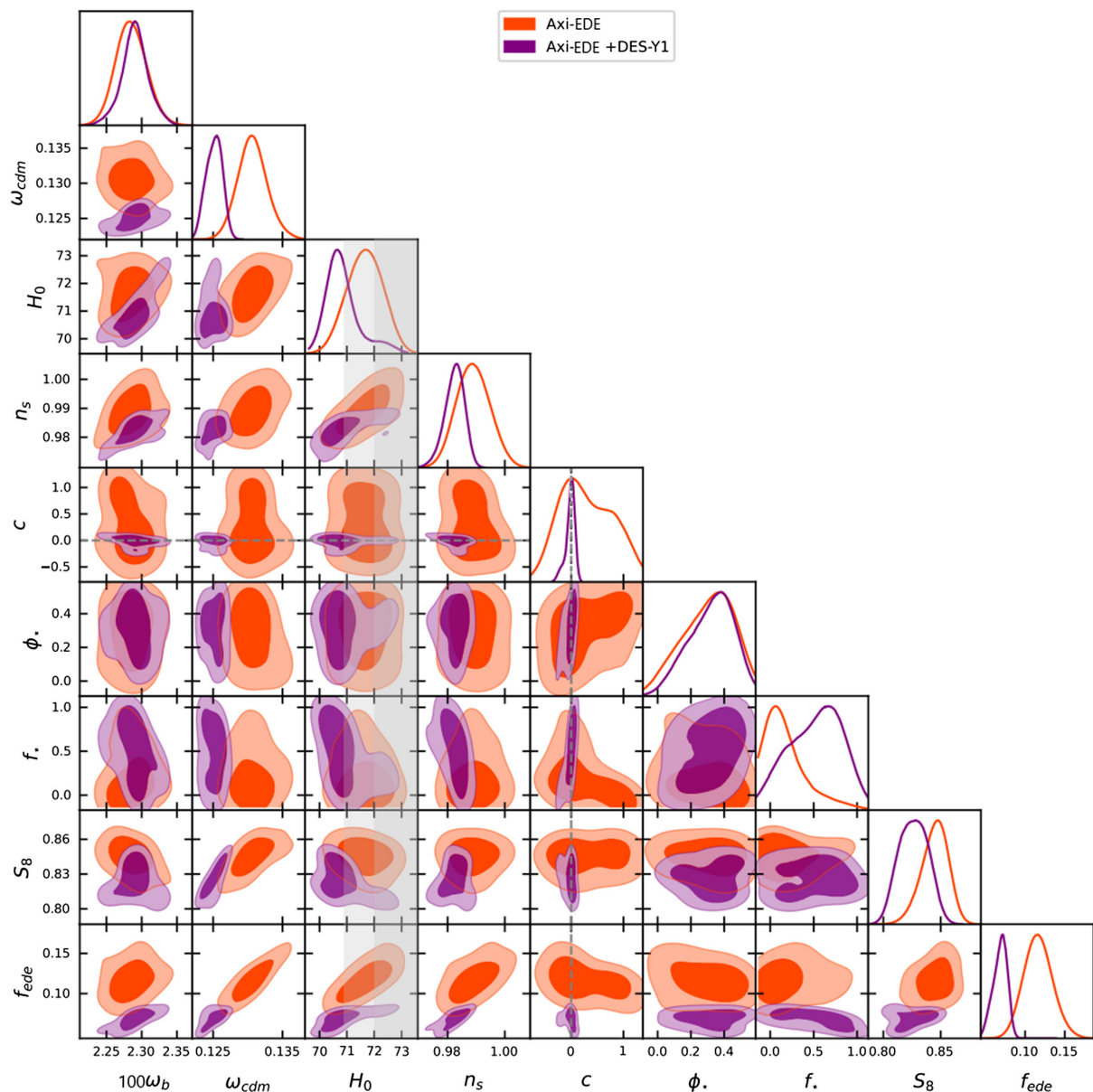


FIG. 4. Posterior distributions for axionlike EDE with coupling (6) in fit to the baseline  $+ H_0$  and the baseline dataset  $+ H_0 + \text{DES-Y1}$  datasets, respectively. The shadows correspond to the  $1\sigma$  and  $2\sigma$  regions of  $H_0$  in light of recent SHOES [2].

$$\dot{\theta} + aH\theta = \frac{1}{\rho_{\text{cdm}}} \frac{d\rho_{\text{cdm}}}{d\phi} (k^2 \delta\phi - \dot{\phi}\theta), \quad (12)$$

where the velocity perturbation  $\theta \equiv \partial_i v^i$ .

The AdS-EDE contains an anti-de Sitter (AdS) vacuum that naturally emerges from the string theory. Instead of oscillating at the bottom of the potential in axion-EDE, the field rolls over the AdS vacuum and climbs up and settles down a cosmological constant  $\Lambda > 0$  region. However, in the AdS-EDE model  $\phi - \phi_i > 0$ , see Fig. 2(b), so  $d\rho_{\text{cdm}}/d\phi = -c\rho_{\text{cdm}}f(\phi)/M_{pl}$ . This suggests that  $\phi_0$  must be obtained by solving the equation of motion, so it is not convenient to use Eq. (9). Integrating Eq. (8), instead we have

$$\begin{aligned}\rho_{\text{cdm}}^{(\text{AdS})}(a) &= \frac{3M_{pl}^2 H_0^2 \Omega_{\text{cdm}}}{a^3} \left[ 1 - f(\phi_0) \right. \\ &\quad \left. + (1 - f(\phi_0)) \frac{f_*}{1 - f_*} \frac{m(\phi)}{m(\phi_i)} \right] \\ &= \frac{3M_{pl}^2 H_0^2 \tilde{\Omega}_{\text{cdm}}}{a^3} \left[ 1 + f_*^{(\text{AdS})} \frac{m(\phi)}{m(\phi_i)} \right],\end{aligned}\quad (13)$$

where  $\tilde{\Omega}_{\text{cdm}} = \Omega_{\text{cdm}}(1 - f(\phi_0))$  is defined to absorb  $\phi_0$  and  $f_*^{(\text{AdS})} = f_*/(1 - f_*)$ .

The changes of parameters  $f_*$  and  $c$  could have some interesting influence on the evolutions of the fraction of

cold dark matter ( $\Omega_{\text{cdm}}$ ) and EDE ( $f_{\text{EDE}}$ ), as shown in Fig. 3. In this coupled EDE model, the dark matter  $\rho_{\text{cdm}} a^3 \propto f_* \exp(-c|\Delta\phi|) + (1 - f_*)$ . The increasing of  $f_*$  and  $c$  both enlarges the difference of initial and present dark matter, lifting the fraction of dark matter in early time with  $\omega_{\text{cdm}}$  fixed. In AdS-EDE, a larger  $c$  corresponds to a stronger coupling of dark matter with EDE, which will cause more decay of dark matter after the field rolls to  $\phi = \phi_0 + \phi_*$ , while a larger  $f_*$  requires the initial density of dark matter larger to keep  $\omega_{\text{cdm}}$  invariant, which contributes to total energy density and causes the decline of  $f_{\text{ede}}$ . In axion-EDE, the effects of  $c$  and  $f_*$  are similar to those in AdS-EDE, though the dark matter decays faster

TABLE II. Mean (bestfit) values of  $\Lambda\text{CDM}$  and AdS-EDE with and without coupling (6) in fit to the baseline, baseline + SH0ES and the baseline + SH0ES + DES-Y1 datasets, respectively.

$\Lambda\text{CDM}$			
Parameters	Baseline	Baseline + $H_0$	Baseline + $H_0$ + DES-Y1
$100\omega_b$	$2.238(2.239) \pm 0.014$	$2.252(2.249) \pm 0.013$	$2.257(2.263) \pm 0.014$
$\omega_{\text{cdm}}$	$0.1179(0.1177) \pm 0.0012$	$0.1182(0.1184) \pm 0.0008$	$0.1172(0.1167) \pm 0.0007$
$H_0$	$68.18(68.13) \pm 0.54$	$68.21(68.16) \pm 0.39$	$69.13(69.48) \pm 0.38$
$\ln(10^{10}A_s)$	$3.028(3.042) \pm 0.013$	$3.052(3.052) \pm 0.015$	$3.046(3.048) \pm 0.015$
$n_s$	$0.9686(0.9687) \pm 0.0044$	$0.9691(0.9686) \pm 0.0035$	$0.9705(0.9769) \pm 0.0036$
$\tau_{\text{reio}}$	$0.075(0.068) \pm 0.013$	$0.0595(0.0594) \pm 0.0073$	$0.0593(0.0618) \pm 0.0080$
$S_8$	$0.8141(0.8142) \pm 0.012$	$0.8140(0.8156) \pm 0.0098$	$0.8067(0.8019) \pm 0.0103$
AdS-EDE (uncoupled)			
Parameters	Baseline	Baseline + $H_0$	Baseline + $H_0$ + DES-Y1
$100\omega_b$	$2.336(2.320) \pm 0.016$	$2.327(2.320) \pm 0.0188$	$2.3381(2.3430) \pm 0.0123$
$\omega_{\text{cdm}}$	$0.1346(0.1340) \pm 0.0016$	$0.1353(0.1338) \pm 0.0019$	$0.1327(0.1325) \pm 0.0013$
$H_0$	$72.60(72.50) \pm 0.65$	$72.64(72.72) \pm 0.75$	$72.42(73.09) \pm 0.38$
$\ln(10^{10}A_s)$	$3.077(3.074) \pm 0.015$	$3.071(3.067) \pm 0.015$	$3.049(3.039) \pm 0.015$
$n_s$	$0.9976(0.9974) \pm 0.0045$	$0.9938(0.9951) \pm 0.0035$	$0.9958(0.9965) \pm 0.0035$
$\tau_{\text{reio}}$	$0.0574(0.0598) \pm 0.0076$	$0.0530(0.0537) \pm 0.0073$	$0.0451(0.0450) \pm 0.0072$
$f_{\text{ede}}$	$0.115(0.107) \pm 0.0050$	$0.1137(0.1081) \pm 0.0061$	$0.1085(0.1098) \pm 0.0040$
$\ln(1 + z_c)$	$8.220(8.213) \pm 0.070$	$8.168(8.169) \pm 0.071$	$8.218(8.140) \pm 0.083$
$S_8$	$0.8575(0.8558) \pm 0.0108$	$0.8608(0.8592) \pm 0.0116$	$0.8403(0.8276) \pm 0.0119$
AdS-EDE			
Parameters	Baseline	Baseline + $H_0$	Baseline + $H_0$ + DES-Y1
$100\omega_b$	$2.336(2.329) \pm 0.013$	$2.328(2.327) \pm 0.014$	$2.334(2.339) \pm 0.019$
$\omega_{\text{cdm}}$	$0.1295(0.1283) \pm 0.0021$	$0.1298(0.1297) \pm 0.0035$	$0.1307(0.1302) \pm 0.0009$
$H_0$	$72.10(72.02) \pm 0.45$	$72.01(72.15) \pm 0.51$	$72.95(73.33) \pm 0.32$
$\ln(10^{10}A_s)$	$3.079(3.071) \pm 0.014$	$3.076(3.084) \pm 0.014$	$3.086(3.095) \pm 0.013$
$n_s$	$0.9967(0.9966) \pm 0.0030$	$0.9963(0.9974) \pm 0.0035$	$0.9988(0.9967) \pm 0.0024$
$\tau_{\text{reio}}$	$0.0581(0.0585) \pm 0.0058$	$0.0579(0.0602) \pm 0.0075$	$0.0624(0.0681) \pm 0.0072$
$f_{\text{ede}}$	$0.1121(0.1027) \pm 0.0067$	$0.1137(0.1089) \pm 0.0062$	$0.1114(0.1081) \pm 0.0059$
$\ln(1 + z_c)$	$8.1632(8.1593) \pm 0.0731$	$8.168(8.169) \pm 0.077$	$8.1570(8.2925) \pm 0.0671$
$c$	$0.392(0.328) \pm 0.455$	$0.367(0.310) \pm 0.434$	$0.069(0.035) \pm 0.109$
$\phi_*$	$0.331(0.321) \pm 0.137$	$0.333(0.333) \pm 0.136$	$0.113(0.023) \pm 0.092$
$f_*$	$0.031(0.010) \pm 0.027$	$0.030(0.008) \pm 0.025$	$0.013(0.015) \pm 0.018$
$S_8$	$0.8544(0.8548) \pm 0.0090$	$0.8554(0.8604) \pm 0.0097$	$0.8470(0.8433) \pm 0.0086$

with larger  $c$ . The change of dark matter fraction results in the corresponding changes of total energy density, and further impacts the  $f_{\text{EDE}}$ . As a result, a positive  $c$  could shrink  $f_{\text{ede}}$  and  $H_0$ , while a larger  $f_*$  could enhance this effect, consistent with the result in Ref. [42]. However, this effect caused by varying  $c$  and  $f$  is more obvious in AdS-EDE than the axion-EDE model, and thus  $c$  and  $f$  would be more tightly constrained in the AdS-EDE model.

#### IV. DATASET AND RESULTS

In recent years, LSS datasets have delivered precise cosmological constraints, and any extension of the standard cosmological model must also satisfy these bounds. In this

work we analyze the EDE scenario taking into account CMB and LSS data in detail. Here, our baseline dataset consists of

- (1) *CMB*: Planck 2018 low-l and high-l TT, TE, EE spectra, and reconstructed CMB lensing spectrum [1, 97, 98].
- (2) *BAO*: The BOSS DR12 [99] with its full covariant matrix for BAO as well as the 6dFGS [100] and MGS of SDSS [101].
- (3) *Supernovae*: The Pantheon dataset [102] comprised of relative luminosity distances of 1048 SNe Ia in the redshift range  $0.01 < z < 2.3$ .

In the studies on the Hubble tension, one usually confronted the  $\Lambda$ CDM model with the CMB, BAO,

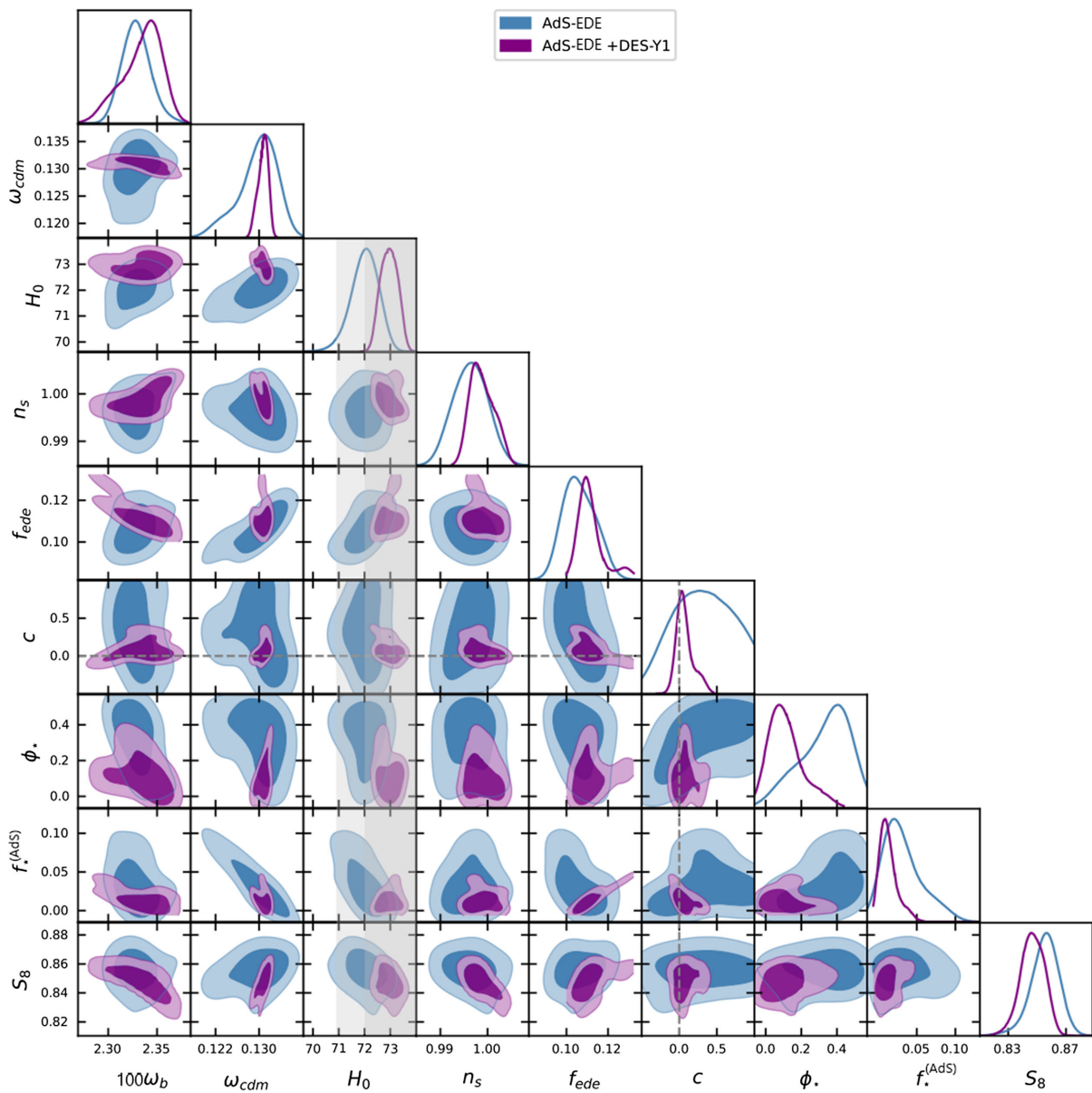


FIG. 5. Posterior distributions for AdS-EDE with coupling (6) in fit to the baseline  $+ H_0$  and the baseline  $+ H_0 + \text{DES-Y1}$  datasets, respectively. The shadows correspond to the  $1\sigma$  and  $2\sigma$  regions of  $H_0$  in light of recent SH0ES [2].

TABLE III.  $\chi^2$  of both axionlike EDE and AdS-EDE for the baseline + SH0ES dataset, where “uncoupled” corresponds to the models without coupling (6).

Dataset	$\Lambda$ CDM	Axion-EDE		AdS-EDE	
		Uncoupled	Uncoupled	Uncoupled	Uncoupled
Planck high-l TT, TE, EE	2347.5	2347.6	2347.33	2347.57	2346.51
Planck low-l EE	398.2	398.19	398.11	397.50	397.42
Planck low-l TT	23.9	20.84	20.92	20.83	20.76
Planck lensing	9.10	10.12	10.04	10.60	9.7
BAO BOSS DR12	1.8	2.24	3.42	2.1	3.53
BAO smallz 2014	2.2	2.06	2.02	2.2	1.77
Pantheon	1026.9	1026.68	1026.87	1026.9	1026.81
SH0ES	22.0	0.27	1.76	0.09	0.73
Total	3831.6	3808.0	3807.7	3807.8	3807.1
$\Delta\chi^2_{\text{SH0ES}}$	0	-21.73	-20.24	-21.91	-21.27
$\Delta\chi^2$	0	-23.6	-23.9	-23.8	-24.5

TABLE IV.  $\chi^2$  of both axionlike EDE and AdS-EDE with coupling (6) for the baseline + SH0ES + DES-Y1 dataset.

Dataset	$\Lambda$ CDM	Axion-EDE	AdS-EDE
Planck high-l TT, TE, EE	2349.41	2347.31	2346.52
Planck low-l EE	398.09	395.82	395.78
Planck low-l TT	21.94	19.25	19.19
Planck lensing	9.26	9.26	9.27
BAO BOSS DR12	3.80	3.94	4.14
BAO smallz 2014	3.32	2.84	2.97
Pantheon	1027.16	1026.96	1026.93
SH0ES	11.7	7.78	0.45
DSE-Y1	517.70	520.90	525.67
Total	4342.38	4334.06	4330.92
$\Delta\chi^2_{\text{SH0ES}}$	0	-3.92	-11.25
$\Delta\chi^2$	0	-8.32	-11.46

Pantheon dataset, so for a comparison we will consider CMB, BAO, Pantheon as our baseline dataset. We add SH0ES prior to baseline for comparison. We also consider the DES-Y1 measurements which are the most statistically powerful LSS data with publicly available likelihoods.

- (4) *SH0ES*: To avoid the *prior volume effect*<sup>1</sup> [103–105], which will compel the EDE models prefer a low  $f_{\text{ede}}$ , we take  $H_0 = 73.04 \pm 1.04 \text{ km/s/Mpc}$  reported by the SH0ES [2] as the Gaussian prior, see also [106,107].
- (5) *DES-Y1*: 26 million galaxies from Dark Energy Survey shape catalogs over  $1321 \text{ deg}^2$  of the southern sky to produce the most significant measurement of cosmic shear in a galaxy survey, including the galaxy angular autocorrelation function of

<sup>1</sup>In the AdS-EDE model, the prior volume effect is actually removed by AdS bound, as explained in [15,22].

650,000 luminous red galaxies in five redshift bins, and the galaxy-shear cross-correlation of luminous red galaxy positions and source galaxy shears [108].

We modified the MontePython-3.3 sampler [109,110] and CLASS codes [111,112]<sup>2</sup> to perform the MCMC analysis for axionlike EDE and AdS-EDE, respectively, with baseline, baseline + SH0ES and baseline + SH0ES + DES-Y1 datasets. We impose broad uniform priors on the  $\Lambda$ CDM parameters, and impose uniform priors on the EDE parameters  $f_{\text{ede}} = [0.001, 0.3]$ , with  $\log_{10}(a_c) = [-4.2, -3.2]$  for axion-EDE and  $\ln(1 + z_c) = [7.5, 9.5]$  for AdS-EDE, and  $\theta_i = [0.1, 3.14]$  where  $\theta_i \equiv \phi/f$  is the initial field displacement in units of the decay constant  $f$  in axion-EDE, and also uniform priors on the coupling parameters  $c = [-2, 2]$  and  $f_* = [0, 1]$ . We simply fix the AdS depth  $\alpha_{\text{ads}}$  to its bestfit value  $\alpha_{\text{ads}} = 3.79 \times 10^{-4}$  to avoid bad convergence of the chain, following the convention in Ref. [11]. Considering the sub-Planckian excursion of the EDE field, we set  $\phi_* = [0, 0.5]$  to enable the coupling to occur. The nuisance parameters of the DES-Y1 dataset are set as displayed in Ref. [108]. The Gelman-Rubin criterion for all chains is converged to  $R - 1 < 0.05$ . We use the “BOBYQA” likelihood maximization method implemented in Cobaya to determine maximum-likelihood parameter values [113–115].

## A. Axionlike EDE

The original EDE model is axionlike EDE [9]. An axion field with  $V(\phi) \propto (1 - \cos[\phi/f])^3$  is responsible for EDE (see recent [116,117] for models in string theory), which starts to oscillate at the redshift  $z_c \sim 3000$ . It is usually parametrized by  $\phi_i$ ,  $a_c$  and  $f_{\text{ede}}$  [9,10]. In Table I, we present the MCMC results for axionlike EDE with the

<sup>2</sup>The corresponding cosmological codes are available: axionlike EDE (<https://github.com/PoulinV/AxiCLASS>) and AdS-EDE ([https://github.com/genye00/class\\_multiscf](https://github.com/genye00/class_multiscf)).

baseline, baseline +  $H_0$  and baseline +  $H_0 + \text{DES-Y1}$  datasets. In Fig. 4, we show the  $1\sigma$  and  $2\sigma$  marginalized posterior distributions of parameter set  $\{\omega_b, \omega_{\text{cdm}}, H_0, \ln(10^{10} A_s), n_s, \tau_{\text{reio}}, \log_{10} a_c, f_{\text{ede}}, \phi_i, c, \phi_*, f_*\}$ .

In contrast to the baseline dataset, the including of  $H_0$  prior primarily lifts  $H_0$  and  $S_8$ , with coupling parameters  $c$  and  $f$  slightly lowered. Though with the baseline +  $H_0$  dataset, we have the bestfit  $S_8 = 0.8438$  (with baseline dataset we have  $S_8 = 0.8425$ ), which is larger than local  $S_8$  measurements, the baseline +  $H_0 + \text{DES-Y1}$  dataset prefers a lower  $S_8$  (the bestfit is  $S_8 = 0.8186$ , which almost equals  $S_8 = 0.8019$  in  $\Lambda\text{CDM}$ ) than that with only the baseline dataset. However, the cost is that the bestfit  $H_0 = 70.14$  is lowered.

In Table I, we see that with baseline and baseline +  $H_0$  dataset,  $c \sim 0$  at  $1\sigma$  region, consistent with the result in Ref. [42], which suggests that such a coupling (4) is not favored, while the case is not altered with the baseline +  $H_0 + \text{DES-Y1}$  dataset. The bestfit of  $c$  is negative and inconsistent with SDC, but the possibility of  $c > 0$  is not ruled out. The coupling lifts the mean values of  $f_{\text{ede}}$ ,  $H_0$ ,

and  $S_8$ , with lower values of bestfits, slightly worsening the  $S_8$  tension. In axionlike EDE with the coupling, the inclusion of DES-Y1 suppresses  $S_8$ , but is still slightly larger than that of  $\Lambda\text{CDM}$ .

## B. AdS-EDE

In the AdS-EDE model [11], we have  $V(\phi) = V_0(\phi/M_p)^4 - V_{\text{ads}}$ , see Fig. 2(b), which is glued to a cosmological constant  $V(\phi) = \Lambda$  by interpolation ( $V_{\text{ads}} > 0$  is the AdS depth). Here, the scalar field starts to roll at the redshift  $z_c \sim 3000$ , and then rolls over an AdS minimum like a fluid with  $w > 1$ . It climbs up to the  $\Lambda > 0$  region shortly after recombination, hereafter the Universe will be effectively described by the  $\Lambda\text{CDM}$  model. It is well known that AdS vacua are ubiquitous in the string landscape, so the AdS-EDE model can be well motivated; see also [118–125] for other studies on the implications of AdS vacua for our Universe.

The AdS-EDE model is usually parametrized by  $V_{\text{ads}}$ ,  $z_c$  and  $f_{\text{ede}}$ . In order to have a significant AdS phase

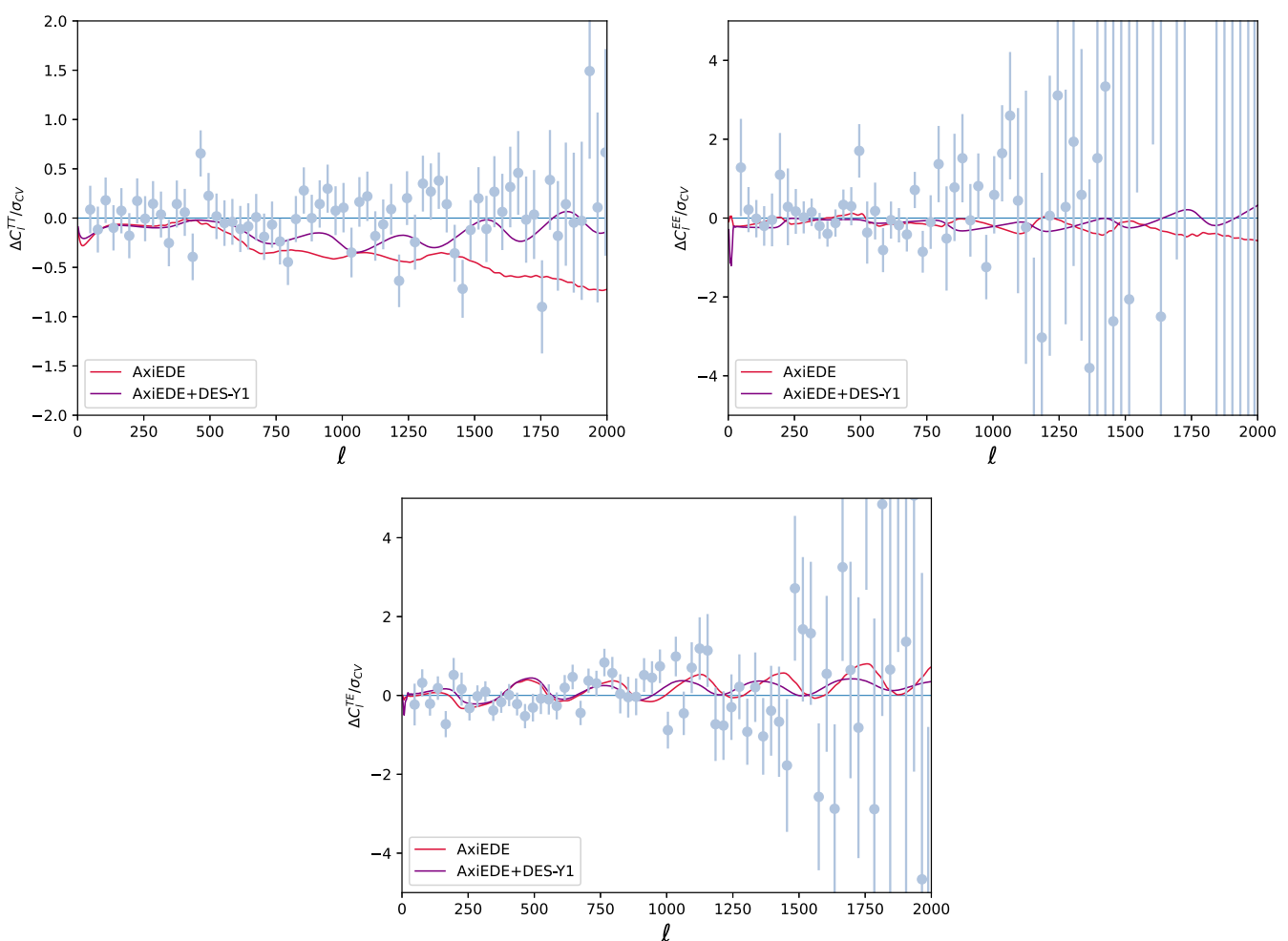


FIG. 6. The TT, EE and TE residuals  $\Delta C_l/\sigma_{cv}$  for the axion-EDE model with coupling (6) in fit to the baseline +  $H_0$  and baseline +  $H_0 + \text{DES-Y1}$  datasets, respectively. The reference model is  $\Lambda\text{CDM}$ .

while making the field able to climb out of the AdS well, we fixed  $V_{\text{ads}}$  by setting  $V_{\text{ads}} = 3.79 \times 10^{-4}(\rho_m(z_c) + \rho_r(z_c))$ , as in Ref. [11]. In Table II, we present the MCMC results for AdS-EDE with the baseline, baseline +  $H_0$  and baseline +  $H_0$  + DES-Y1 datasets. In Fig. 5, we show the  $1\sigma$  and  $2\sigma$  marginalized posterior distributions of parameter set  $\{\omega_b, \omega_{\text{cdm}}, H_0, \ln(10^{10}A_s), n_s, \tau_{\text{reio}}, \ln(1+z_c), f_{\text{ede}}, c, \phi_*, f_*\}$ .

Here, the inclusion of  $H_0$  prior has a similar impact on  $c$  and  $f$  and the inclusion of DES-Y1 has a similar impact on  $S_8$  as in axion-EDE. Though the baseline +  $H_0$  + DES-Y1 dataset prefers a lower  $S_8$  (the bestfit is  $S_8 = 0.8433$ ) than that with only the baseline +  $H_0$  dataset, it is still larger than that in  $\Lambda\text{CDM}$ . However, unlike in axionlike EDE,  $f_{\text{ede}}$  is not suppressed by the coupling (4), since  $f_* \sim 0.02$  is fairly small. It is also noted that with the baseline +  $H_0$  + DES-Y1 dataset, we have the bestfit  $H_0 = 73.33$ , which is slightly higher than that in AdS-EDE [11].

In Table I, we see that with baseline and baseline +  $H_0$  datasets,  $c \sim 0.4$  at the  $1\sigma$  region, which is different from that in axionlike EDE (see Sec. III A) and consistent with SDC, and with the baseline +  $H_0$  + DES-Y1 dataset  $c \gtrsim 0.1$  at  $1\sigma$  region. However, in both cases  $c \sim 0$  is still  $1\sigma$  consistent. In AdS-EDE,  $f_* \sim 0.03$  is smaller than that in axionlike EDE, and  $f_* = 1$  is ruled out at  $2\sigma$ . In AdS-EDE with the coupling, the case is similar to that in axionlike EDE. However,  $S_8$  decreases slightly as  $H_0$  grows with DES-Y1 included, implemented by the changes of three coupling parameters.

We list the  $\chi^2$  of bestfit points for axionlike EDE and AdS-EDE models in Tables III and IV, respectively. In Table III, only with the baseline +  $H_0$  dataset, we see that both models have improvements over the bestfit  $\Lambda\text{CDM}$  by  $\Delta\chi^2 \sim -23$ , where the  $\chi^2$  of Planck low-l TT, EE and  $H_0$  are significantly improved while the  $\chi^2$  of BAO is slightly exacerbated. In Table IV with the baseline + DES-Y1 dataset, we see that both models have improvements over

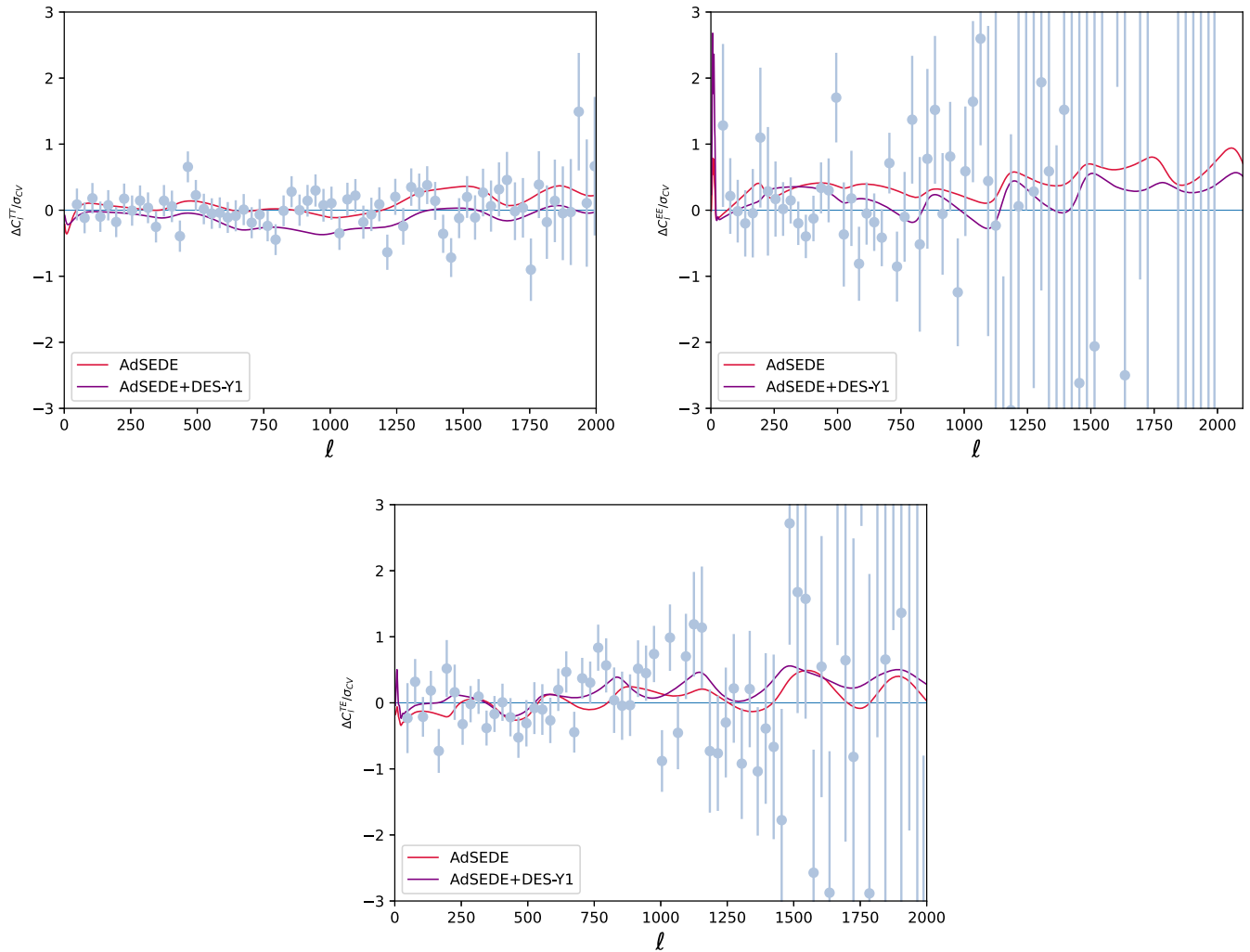


FIG. 7. The TT, EE and TE residuals  $\Delta C_l/\sigma_{CV}$  for the AdS-EDE model with coupling (6) in fit to the baseline +  $H_0$  and baseline +  $H_0$  + DES-Y1 datasets, respectively. The reference model is  $\Lambda\text{CDM}$ .

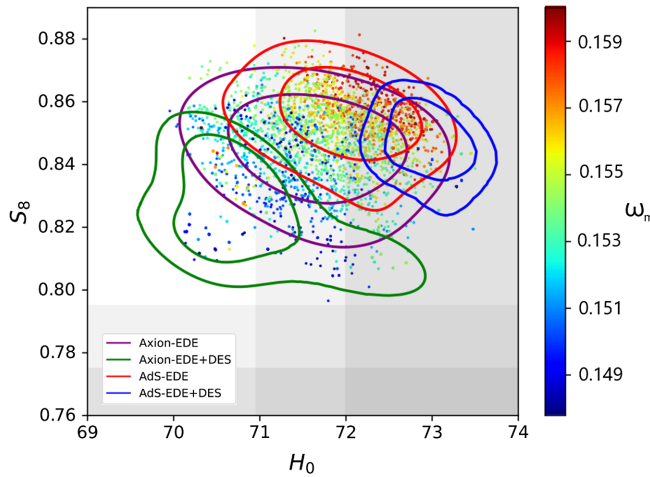


FIG. 8. The  $S_8 - H_0$  contour of axionlike EDE and AdS-EDE with the coupling (6) in fit to the baseline and baseline + DES-Y1 datasets, respectively. The shadows correspond to the  $1\sigma$  and  $2\sigma$  regions of  $H_0$  in light of recent SH0ES  $H_0 = 73.04 \pm 1.04$  km/s/Mpc [2] and  $S_8$  in light of KiDS + VIKING-450 + DES-Y1 constraint  $S_8 = 0.755 \pm 0.02$  [28].

the bestfit  $\Lambda$ CDM but by only  $\Delta\chi^2 \sim -10$ . In both axionlike EDE and AdS-EDE models, compared with  $\Lambda$ CDM, the  $\chi^2$  of DES-Y1 is exacerbated with  $\Delta\chi^2 \sim +3$  and  $\Delta\chi^2 \sim +8$ , respectively. Although the decrease of  $\chi^2$  is mainly contributed by the fit to SH0ES, the coupled AdS-EDE model permits a large  $H_0$  and DES-Y1 coexisting by adjusting  $c$  and  $f$ , with exacerbating the fit to BAO.

We also plot the TT, EE and TE residuals  $\Delta C_l = C_{l,\text{model}} - C_{l,\Lambda}$  of both models in units of the cosmic variance per multipole

$$\sigma_{CV} = \begin{cases} \sqrt{2/(2l+1)}C_l^{\text{TT}}, & \text{TT} \\ \sqrt{1/(2l+1)}\sqrt{C_l^{\text{TT}}C_l^{\text{EE}} + (C_l^{\text{TE}})^2}, & \text{TE} \\ \sqrt{2/(2l+1)}C_l^{\text{EE}}, & \text{EE} \end{cases}$$

in Figs. 6 and 7. The TT residual becomes comparable to  $\sigma_{CV}$  at  $l \sim 700$  for axionlike EDE. The first peak of

axion-EDE becomes unobvious after coupling to dark matter with a significant difference at  $l > 1000$ . In AdS-EDE the coupling retains the lowering at  $l \sim 1000$  in the TT spectrum and the bump around  $l \sim 200$  in the EE spectrum, while increasing the amplitude as  $l$  becomes large. In the EE spectrum, the deviations oscillate around zero slightly below  $l \sim 1000$ , but have little statistical weight when comparing the fit to  $\Lambda$ CDM. We can see that the EDE curves of the EE spectrum both have a shift upwards at  $l < 250$  and  $500 < l < 1000$  providing a slightly better fit to the data there than CDM.

The signals are suppressed both in TT and TE spectrums, corresponding to a lower  $S_8$  value.

## V. HAS DM EVER FADED?

In Fig. 8, we see that the smaller  $S_8$  caused by the DES-Y1 dataset brought with a lower bestfit  $\omega_{\text{cdm}} = 0.1236$  and  $H_0 = 70.14$  for axionlike EDE, but a higher bestfit  $\omega_{\text{cdm}} = 0.1302$  and  $H_0 = 73.33$  for AdS-EDE. Thus though (3) is still right for both models with the coupling (6), such a coupling actually impairs the correlation between  $\omega_m$  and  $S_8$ , so that the rise of  $H_0$  must not be accompanied with the exacerbation of  $S_8$  tension.

Though in axionlike EDE and AdS-EDE models  $c = 0$  is  $1\sigma$  consistent, however, the  $1\sigma$  contour of  $c$  is wide so that  $c \gtrsim 0.1$  is also allowed due to a small  $f_*$ , see Table I. In Fig. 9, we plot the evolution of the scalar field,  $f_{\text{ede}}$ , and the mass  $m_{\text{cdm}}(\phi)$  of DM in both models with their bestfit values. The baseline +  $H_0$  dataset allows a higher  $c \gtrsim 0.1$ , so a larger shift of  $m_{\text{cdm}}(\phi)$ , which suggests that a small fraction of DM ( $f_* \sim 0.2$  and  $f_* \sim 0.03$  for both models) will fade with EDE. However, it should be mentioned that in axionlike EDE the bestfit of  $c \sim 0$  is a negative value, consistent with the result in Ref. [42].

However, after the DES-Y1 dataset included, we have  $c \sim 0$  further, particularly for axionlike EDE with a smaller excursion of scalar field and a lower  $f_{\text{ede}}$ . Thus, in both the axionlike EDE and AdS-EDE models the fading of DM is actually not favored by the baseline +  $H_0$  + DES-Y1 dataset, but it cannot be ruled out at present.

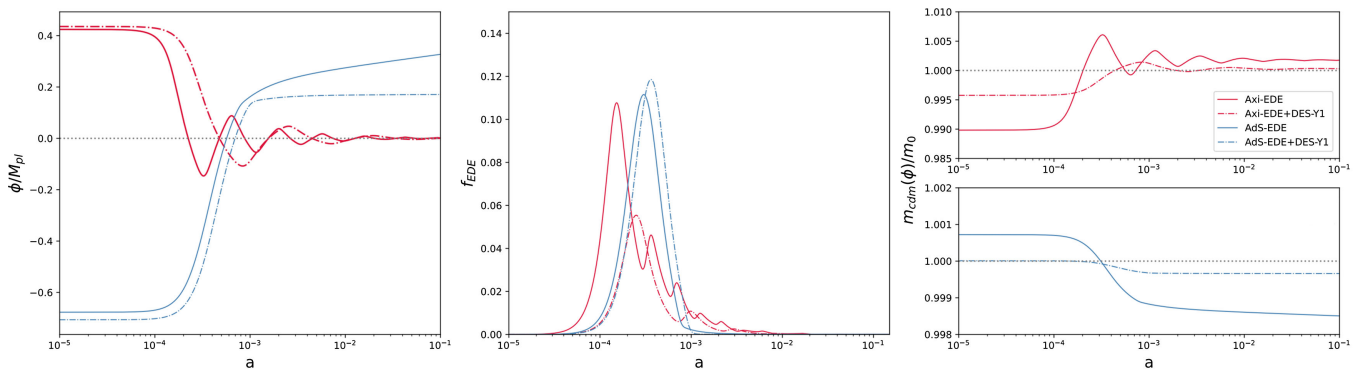


FIG. 9. The evolutions of the scalar field,  $f_{\text{ede}}$  and  $m_{\text{cdm}}(\phi)$  in axionlike EDE and AdS-EDE models with their bestfit values.

## VI. CONCLUSIONS

Inspired by SDC, we investigated the impact of DM fractionally coupled to EDE, especially the possibility of resolving  $S_8$  tension. We performed the MCMC analysis for axionlike EDE and AdS-EDE, respectively, with PlanckCMB, BAO, Pantheon dataset (our baseline dataset), as well as and SHOES and DES-Y1 datasets.

It is found that the  $S_8$  tension can be alleviated with such a fractional coupling. In the axionlike EDE model, the baseline + SHOES + DES-Y1 dataset prefers a lower  $S_8$  (the bestfit is  $S_8 \simeq 0.82$ , which almost equals to  $S_8 = 0.8156$  in  $\Lambda$ CDM), however, the cost is a lower bestfit  $H_0 = 70.14$ , while in the AdS-EDE model, though the baseline + SHOES + DES-Y1 dataset prefers a lower  $S_8$  (the bestfit is  $S_8 = 0.8433$ ), it is still larger than that in  $\Lambda$ CDM.

The baseline + SHOES + DES-Y1 dataset allows  $c \gtrsim 0.1$  in both EDE models due to a small  $f_* \ll 1$  (bestfit  $f \sim 0.5$  for axionlike EDE while a smaller  $f_* \sim 0.02$  for AdS-EDE), which is compatible with SDC and suggests that a small fraction of DM has ever faded with EDE. However,  $c \sim 0$  is still at the  $1\sigma$  region, particularly in axionlike EDE the bestfit of  $c$  is a negative value, consistent with the result in Ref. [42].

It is worth mentioning that in EDE models with fullPlanck + BAO + Pantheon dataset, the shift of primordial scalar spectral index scales as  $\delta n_s \simeq 0.4 \frac{\delta H_0}{H_0}$  [126],

which suggests a scale-invariant Harrison-Zeldovich spectrum ( $n_s = 1$ ) for  $H_0 \sim 73$  km/s/Mpc.<sup>3</sup> In Refs. [19,20], with Planck + ACT + SPT + BAO + Pantheon dataset, similar results have also been found. Here, we observed that the *preference* for  $n_s = 1$  is not altered by the inclusion of the large-scale structure DES-Y1 dataset (see recent [127] for BOSS dataset), see Tables I and II. In this sense, the Hubble tension seems to hint that we might live in a scale-free Universe, so it is interesting to think about how  $n_s = 1$  would dramatically impact our understanding on the primordial Universe and inflation [126,128–133].

## ACKNOWLEDGMENTS

We thank Gen Ye and Jun-Qian Jiang for helpful discussions. H. W. is supported by UCAS Undergraduate Innovative Practice Project. Y. S. P. is supported by the NSFC, No. 12075246, and by the Fundamental Research Funds for the Central Universities. We acknowledge the use of publicly available codes AXICLASS [134] and CLASSMULTISCF [135].

<sup>3</sup>See [22] for the Planck + BICEP/Keck dataset, in which the  $r - n_s$  contour for EDE was first shown ( $r$  is the tensor-to-scalar ratio).

- 
- [1] N. Aghanim *et al.* (Planck Collaboration), *Astron. Astrophys.* **641**, A6 (2020); **652**, C4(E) (2021).
- [2] A. G. Riess, W. Yuan, L. M. Macri, D. Scolnic, D. Brout, S. Casertano, D. O. Jones, Y. Murakami, L. Breuval, T. G. Brink *et al.*, *Astrophys. J. Lett.* **934**, L7 (2022).
- [3] L. Verde, T. Treu, and A. G. Riess, *Nat. Astron.* **3**, 891 (2019).
- [4] A. G. Riess, *Nat. Rev. Phys.* **2**, 10 (2019).
- [5] L. Knox and M. Millea, *Phys. Rev. D* **101**, 043533 (2020).
- [6] E. Di Valentino, O. Mena, S. Pan, L. Visinelli, W. Yang, A. Melchiorri, D. F. Mota, A. G. Riess, and J. Silk, *Classical Quantum Gravity* **38**, 153001 (2021).
- [7] L. Perivolaropoulos and F. Skara, *New Astron. Rev.* **95**, 101659 (2022).
- [8] T. Karwal and M. Kamionkowski, *Phys. Rev. D* **94**, 103523 (2016).
- [9] V. Poulin, T. L. Smith, T. Karwal, and M. Kamionkowski, *Phys. Rev. Lett.* **122**, 221301 (2019).
- [10] T. L. Smith, V. Poulin, and M. A. Amin, *Phys. Rev. D* **101**, 063523 (2020).
- [11] G. Ye and Y. S. Piao, *Phys. Rev. D* **101**, 083507 (2020).
- [12] G. Ye and Y. S. Piao, *Phys. Rev. D* **102**, 083523 (2020).
- [13] A. Chudaykin, D. Gorbunov, and N. Nedelko, *J. Cosmol. Astropart. Phys.* **08** (2020) 013.
- [14] A. Chudaykin, D. Gorbunov, and N. Nedelko, *Phys. Rev. D* **103**, 043529 (2021).
- [15] J. Q. Jiang and Y. S. Piao, *Phys. Rev. D* **104**, 103524 (2021).
- [16] J. C. Hill, E. Calabrese, S. Aiola, N. Battaglia, B. Bolliet, S. K. Choi, M. J. Devlin, A. J. Duivenvoorden, J. Dunkley, S. Ferraro *et al.*, *Phys. Rev. D* **105**, 123536 (2022).
- [17] V. Poulin, T. L. Smith, and A. Bartlett, *Phys. Rev. D* **104**, 123550 (2021).
- [18] A. La Posta, T. Louis, X. Garrido, and J. C. Hill, *Phys. Rev. D* **105**, 083519 (2022).
- [19] T. L. Smith, M. Lucca, V. Poulin, G. F. Abellán, L. Balkenhol, K. Benabed, S. Galli, and R. Murgia, *Phys. Rev. D* **106**, 043526 (2022).
- [20] J. Q. Jiang and Y. S. Piao, *Phys. Rev. D* **105**, 103514 (2022).
- [21] J. S. Cruz, F. Niedermann, and M. S. Sloth, *J. Cosmol. Astropart. Phys.* **02** (2023) 041.
- [22] G. Ye and Y. S. Piao, *Phys. Rev. D* **106**, 043536 (2022).
- [23] J. C. Hill, E. McDonough, M. W. Toomey, and S. Alexander, *Phys. Rev. D* **102**, 043507 (2020).
- [24] M. M. Ivanov, E. McDonough, J. C. Hill, M. Simonović, M. W. Toomey, S. Alexander, and M. Zaldarriaga, *Phys. Rev. D* **102**, 103502 (2020).

- [25] G. D’Amico, L. Senatore, P. Zhang, and H. Zheng, *J. Cosmol. Astropart. Phys.* **05** (2021) 072.
- [26] C. Krishnan, E. Ó. Colgáin, Ruchika, A. A. Sen, M. M. Sheikh-Jabbari, and T. Yang, *Phys. Rev. D* **102**, 103525 (2020).
- [27] R. C. Nunes and S. Vagnozzi, *Mon. Not. R. Astron. Soc.* **505**, 5427 (2021).
- [28] M. Asgari, T. Tröster, C. Heymans, H. Hildebrandt, J. L. van den Busch, A. H. Wright, A. Choi, T. Erben, B. Joachimi, S. Joudaki *et al.*, *Astron. Astrophys.* **634**, A127 (2020).
- [29] M. Asgari *et al.* (KiDS Collaboration), *Astron. Astrophys.* **645**, A104 (2021).
- [30] T. M. C. Abbott *et al.* (DES Collaboration), *Phys. Rev. D* **105**, 023520 (2022).
- [31] V. Poulin, J. L. Bernal, E. Kovetz, and M. Kamionkowski, *Phys. Rev. D* **107**, 123538 (2023).
- [32] I. J. Allali, M. P. Hertzberg, and F. Rompineve, *Phys. Rev. D* **104**, L081303 (2021).
- [33] G. Ye, J. Zhang, and Y. S. Piao, *Phys. Lett. B* **839**, 137770 (2023).
- [34] S. Alexander, H. Bernardo, and M. W. Toomey, *J. Cosmol. Astropart. Phys.* **03** (2023) 037.
- [35] G. Franco Abellán, R. Murgia, and V. Poulin, *Phys. Rev. D* **104**, 123533 (2021).
- [36] S. J. Clark, K. Vattis, J. Fan, and S. M. Koushiappas, *Phys. Rev. D* **107**, 083527 (2023).
- [37] T. Simon, G. Franco Abellán, P. Du, V. Poulin, and Y. Tsai, *Phys. Rev. D* **106**, 023516 (2022).
- [38] A. Reeves, L. Herold, S. Vagnozzi, B. D. Sherwin, and E. G. M. Ferreira, *Mon. Not. R. Astron. Soc.* **520**, 3688 (2023).
- [39] Z. Chacko, Y. Cui, S. Hong, T. Okui, and Y. Tsai, *J. High Energy Phys.* **12** (2016) 108.
- [40] M. A. Buen-Abad, Z. Chacko, C. Kilic, G. Marques-Tavares, and T. Youn, *J. High Energy Phys.* **06** (2023) 012.
- [41] T. Karwal, M. Raveri, B. Jain, J. Khoury, and M. Trodden, *Phys. Rev. D* **105**, 063535 (2022).
- [42] E. McDonough, M. X. Lin, J. C. Hill, W. Hu, and S. Zhou, *Phys. Rev. D* **106**, 043525 (2022).
- [43] K. V. Berghaus and T. Karwal, *Phys. Rev. D* **107**, 103515 (2023).
- [44] J. Sakstein and M. Trodden, *Phys. Rev. Lett.* **124**, 161301 (2020).
- [45] M. Carrillo González, Q. Liang, J. Sakstein, and M. Trodden, *J. Cosmol. Astropart. Phys.* **04** (2021) 063.
- [46] G. Ballesteros, A. Notari, and F. Rompineve, *J. Cosmol. Astropart. Phys.* **11** (2020) 024.
- [47] M. Braglia, M. Ballardini, W. T. Emond, F. Finelli, A. E. Gumrukcuoglu, K. Koyama, and D. Paoletti, *Phys. Rev. D* **102**, 023529 (2020).
- [48] M. Braglia, M. Ballardini, F. Finelli, and K. Koyama, *Phys. Rev. D* **103**, 043528 (2021).
- [49] T. Adi and E. D. Kovetz, *Phys. Rev. D* **103**, 023530 (2021).
- [50] A. Gómez-Valent, Z. Zheng, L. Amendola, C. Wetterich, and V. Pettorino, *Phys. Rev. D* **106**, 103522 (2022).
- [51] H. Ooguri and C. Vafa, *Nucl. Phys.* **B766**, 21 (2007).
- [52] P. Agrawal, G. Obied, and C. Vafa, *Phys. Rev. D* **103**, 043523 (2021).
- [53] T. L. Smith, V. Poulin, and T. Simon, arXiv:2208.12992.
- [54] N. Kaloper, *Int. J. Mod. Phys. D* **28**, 1944017 (2019).
- [55] P. Agrawal, F. Y. Cyr-Racine, D. Pinner, and L. Randall, arXiv:1904.01016.
- [56] S. Alexander and E. McDonough, *Phys. Lett. B* **797**, 134830 (2019).
- [57] K. V. Berghaus and T. Karwal, *Phys. Rev. D* **101**, 083537 (2020).
- [58] M. X. Lin, G. Benevento, W. Hu, and M. Raveri, *Phys. Rev. D* **100**, 063542 (2019).
- [59] M. Braglia, W. T. Emond, F. Finelli, A. E. Gumrukcuoglu, and K. Koyama, *Phys. Rev. D* **102**, 083513 (2020).
- [60] M. X. Lin, W. Hu, and M. Raveri, *Phys. Rev. D* **102**, 123523 (2020).
- [61] O. Seto and Y. Toda, *Phys. Rev. D* **103**, 123501 (2021).
- [62] S. Nojiri, S. D. Odintsov, D. Saez-Chillon Gomez, and G. S. Sharov, *Phys. Dark Universe* **32**, 100837 (2021).
- [63] S. Nojiri, S. D. Odintsov, and V. K. Oikonomou, *Nucl. Phys.* **B980**, 115850 (2022).
- [64] H. Mohseni Sadjadi and V. Anari, *Eur. Phys. J. Plus* **138**, 84 (2023).
- [65] V. I. Sabla and R. R. Caldwell, *Phys. Rev. D* **106**, 063526 (2022).
- [66] M. X. Lin, M. Raveri, and W. Hu, *Phys. Rev. D* **99**, 043514 (2019).
- [67] J. Solà Peracaula, A. Gómez-Valent, J. de Cruz Pérez, and C. Moreno-Pulido, *Astrophys. J. Lett.* **886**, L6 (2019).
- [68] M. Zumalacarregui, *Phys. Rev. D* **102**, 023523 (2020).
- [69] J. Solà Peracaula, A. Gómez-Valent, J. de Cruz Pérez, and C. Moreno-Pulido, *Classical Quantum Gravity* **37**, 245003 (2020).
- [70] T. Fujita, K. Murai, H. Nakatsuka, and S. Tsujikawa, *Phys. Rev. D* **103**, 043509 (2021).
- [71] K. Murai, F. Naokawa, T. Namikawa, and E. Komatsu, *Phys. Rev. D* **107**, L041302 (2023).
- [72] M. Braglia and S. Kuroyanagi, *Phys. Rev. D* **104**, 123547 (2021).
- [73] C. F. Chang, *Phys. Rev. D* **105**, 023508 (2022).
- [74] H. Wang and Y. S. Piao, *Phys. Lett. B* **832**, 137244 (2022).
- [75] E. Di Valentino, A. Melchiorri, E. V. Linder, and J. Silk, *Phys. Rev. D* **96**, 023523 (2017).
- [76] S. Vagnozzi, *Phys. Rev. D* **102**, 023518 (2020).
- [77] E. Di Valentino, A. Melchiorri, O. Mena, and S. Vagnozzi, *Phys. Dark Universe* **30**, 100666 (2020).
- [78] W. Yang, E. Di Valentino, S. Pan, and O. Mena, *Phys. Dark Universe* **31**, 100762 (2021).
- [79] W. Yang, E. Di Valentino, S. Pan, Y. Wu, and J. Lu, *Mon. Not. R. Astron. Soc.* **501**, 5845 (2021).
- [80] M. G. Dainotti, B. De Simone, T. Schiavone, G. Montani, E. Rinaldi, and G. Lambiase, *Astrophys. J.* **912**, 150 (2021).
- [81] G. Alestas, D. Camarena, E. Di Valentino, L. Kazantzidis, V. Marra, S. Nesseris, and L. Perivolaropoulos, *Phys. Rev. D* **105**, 063538 (2022).
- [82] M. G. Dainotti, B. De Simone, T. Schiavone, G. Montani, E. Rinaldi, G. Lambiase, M. Bogdan, and S. Ugale, *Galaxies* **10**, 24 (2022).
- [83] L. Heisenberg, H. Villarrubia-Rojo, and J. Zosso, *Phys. Rev. D* **106**, 043503 (2022).
- [84] R. C. Nunes, S. Vagnozzi, S. Kumar, E. Di Valentino, and O. Mena, *Phys. Rev. D* **105**, 123506 (2022).

- [85] T. Schiavone, G. Montani, M. G. Dainotti, B. De Simone, E. Rinaldi, and G. Lambiase, [arXiv:2205.07033](https://arxiv.org/abs/2205.07033).
- [86] W. Liu, L. A. Anchordoqui, E. Di Valentino, S. Pan, Y. Wu, and W. Yang, *J. Cosmol. Astropart. Phys.* **02** (2022) 012.
- [87] C. Krishnan, R. Mohayaee, E. Ó. Colgáin, M. M. Sheikh-Jabbari, and L. Yin, *Classical Quantum Gravity* **38**, 184001 (2021).
- [88] L. Perivolaropoulos and F. Skara, *Phys. Rev. D* **104**, 123511 (2021).
- [89] S. D. Odintsov and V. K. Oikonomou, *Europhys. Lett.* **137**, 39001 (2022).
- [90] S. D. Odintsov and V. K. Oikonomou, *Europhys. Lett.* **139**, 59003 (2022).
- [91] V. K. Oikonomou, P. Tsyba, and O. Razina, *Universe* **8**, 484 (2022).
- [92] C. Krishnan, E. Ó. Colgáin, M. M. Sheikh-Jabbari, and T. Yang, *Phys. Rev. D* **103**, 103509 (2021).
- [93] E. Ó. Colgáin, M. M. Sheikh-Jabbari, R. Solomon, G. Bargiacchi, S. Capozziello, M. G. Dainotti, and D. Stojkovic, *Phys. Rev. D* **106**, L041301 (2022).
- [94] E. Ó. Colgáin, M. M. Sheikh-Jabbari, R. Solomon, M. G. Dainotti, and D. Stojkovic, [arXiv:2206.11447](https://arxiv.org/abs/2206.11447).
- [95] T. D. Brennan, F. Carta, and C. Vafa, *Proc. Sci. TASI2017 (2017)* 015.
- [96] E. Palti, *Fortschr. Phys.* **67**, 1900037 (2019).
- [97] N. Aghanim *et al.* (Planck Collaboration), *Astron. Astrophys.* **641**, A5 (2020).
- [98] N. Aghanim *et al.* (Planck Collaboration), *Astron. Astrophys.* **641**, A8 (2020).
- [99] S. Alam *et al.* (BOSS Collaboration), *Mon. Not. R. Astron. Soc.* **470**, 2617 (2017).
- [100] F. Beutler, C. Blake, M. Colless, D. H. Jones, L. Staveley-Smith, L. Campbell, Q. Parker, W. Saunders, and F. Watson, *Mon. Not. R. Astron. Soc.* **416**, 3017 (2011).
- [101] A. J. Ross, L. Samushia, C. Howlett, W. J. Percival, A. Burden, and M. Manera, *Mon. Not. R. Astron. Soc.* **449**, 835 (2015).
- [102] D. M. Scolnic *et al.* (Pan-STARRS1 Collaboration), *Astrophys. J.* **859**, 101 (2018).
- [103] N. Schöneberg, G. Franco Abellán, A. Pérez Sánchez, S. J. Witte, V. Poulin, and J. Lesgourgues, *Phys. Rep.* **984**, 1 (2022).
- [104] L. Herold, E. G. M. Ferreira, and E. Komatsu, *Astrophys. J. Lett.* **929**, L16 (2022).
- [105] A. Gómez-Valent, *Phys. Rev. D* **106**, 063506 (2022).
- [106] D. Camarena and V. Marra, *Mon. Not. R. Astron. Soc.* **504**, 5164 (2021).
- [107] G. Efstathiou, *Mon. Not. R. Astron. Soc.* **505**, 3866 (2021).
- [108] T. M. C. Abbott *et al.* (DES Collaboration), *Phys. Rev. D* **98**, 043526 (2018).
- [109] B. Audren, J. Lesgourgues, K. Benabed, and S. Prunet, *J. Cosmol. Astropart. Phys.* **02** (2013) 001.
- [110] T. Brinckmann and J. Lesgourgues, *Phys. Dark Universe* **24**, 100260 (2019).
- [111] J. Lesgourgues, [arXiv:1104.2932](https://arxiv.org/abs/1104.2932).
- [112] D. Blas, J. Lesgourgues, and T. Tram, *J. Cosmol. Astropart. Phys.* **07** (2011) 034.
- [113] C. Cartis, J. Fiala, B. Marteau, and L. Roberts, [arXiv:1804.00154](https://arxiv.org/abs/1804.00154).
- [114] C. Cartis, L. Roberts, and O. Sheridan-Methven, *Optimization* **71**, 2343 (2022).
- [115] M. Powell, The bobyqa algorithm for bound constrained optimization without derivatives, Report No. NA2009/06, University of Cambridge, Cambridge (2009).
- [116] E. McDonough and M. Scalisi, [arXiv:2209.00011](https://arxiv.org/abs/2209.00011).
- [117] K. Kojima and Y. Okubo, *Phys. Rev. D* **106**, 063540 (2022).
- [118] K. Dutta, Ruchika, A. Roy, A. A. Sen, and M. M. Sheikh-Jabbari, *Gen. Relativ. Gravit.* **52**, 15 (2020).
- [119] L. Visinelli, S. Vagnozzi, and U. Danielsson, *Symmetry* **11**, 1035 (2019).
- [120] Ö. Akarsu, J. D. Barrow, L. A. Escamilla, and J. A. Vazquez, *Phys. Rev. D* **101**, 063528 (2020).
- [121] R. Calderón, R. Gannouji, B. L'Huillier, and D. Polarski, *Phys. Rev. D* **103**, 023526 (2021).
- [122] Ö. Akarsu, S. Kumar, E. Özülker, and J. A. Vazquez, *Phys. Rev. D* **104**, 123512 (2021).
- [123] A. A. Sen, S. A. Adil, and S. Sen, *Mon. Not. R. Astron. Soc.* **518**, 1098 (2022).
- [124] S. Di Gennaro and Y. C. Ong, *Universe* **8**, 541 (2022).
- [125] H. Moshafi, H. Firouzjahi, and A. Talebian, *Astrophys. J.* **940**, 121 (2022).
- [126] G. Ye, B. Hu, and Y. S. Piao, *Phys. Rev. D* **104**, 063510 (2021).
- [127] T. Simon, P. Zhang, V. Poulin, and T. L. Smith, *Phys. Rev. D* **107**, 063505 (2023).
- [128] G. D'Amico, N. Kaloper, and A. Westphal, *Phys. Rev. D* **105**, 103527 (2022).
- [129] R. Kallosh and A. Linde, *Phys. Rev. D* **106**, 023522 (2022).
- [130] C. M. Lin, *Phys. Rev. D* **106**, 103511 (2022).
- [131] G. Ye, J. Q. Jiang, and Y. S. Piao, *Phys. Rev. D* **106**, 103528 (2022).
- [132] Y. Ageeva, P. Petrov, and V. Rubakov, *J. High Energy Phys.* **01** (2023) 026.
- [133] G. D'Amico and N. Kaloper, *Phys. Rev. D* **106**, 103503 (2022).
- [134] <https://github.com/PoulinV/AxiCLASS>.
- [135] [https://github.com/genye00/class\\_multiscf.git](https://github.com/genye00/class_multiscf.git).